Chemical Physics Letters 649 (2016) 103–110

Contents lists available at ScienceDirect

Chemical Physics Letters

journal homepage: www.elsevier.com/locate/cplett

A DFT-chemotopological study on the 3D transition metal oxides and dioxygen complexes

Daniel E. Trujillo-González [a], María C. Ramírez-Romero [a], Juan I. Rodríguez [b], Emilbus A. Uribe [a,*]

[a] Departamento de Ciencias Básicas, Universidad Santo Tomás, Carrera 9, No. 51-11, Bogotá, Colombia
[b] Escuela Superior de Física y Matemáticas, Instituto Politécnico Nacional, Edificio 9, U.P.A.L.M., Col. San Pedro Zacatenco, C.P. 07738, México, D.F., Mexico

ARTICLE INFO

Article history:
Received 8 July 2015
In final form 9 February 2016
Available online 22 February 2016

ABSTRACT

Density functional theory unrestricted calculations at the BPW91/6-311+G* level of theory have been used to explore the potential energy surface of MO_n complexes (M = Sc–Zn, n = 1–2). Nine physico-chemical properties were selected to characterize each of the MO_n complexes to conduct a chemotopological study. Our results show that the similarity relations between the group-VIIIB elements (Fe, Co and Ni) are transferred to their corresponding MO_n complexes. A classification of M—O interactions in the MO_n complexes based on the QTAIM methodology is introduced.

1. Introduction

Transition metal oxides and dioxides are potential intermediates/products during oxidation of metal atoms and clusters [1]. In particular, fourth-period transition metal oxides and dioxides play an important role in some biological [2] and catalytic processes [1]. Structural and physico-chemical properties of these molecules have been studied experimentally and theoretically [1,3–5]. Yet detailed information on the bonding between the transition metal and oxygen remains to be elucidated.

The fourth-period transition metals (M) can interact with the O_2 ligand to form oxo and dioxygen complexes [1]. The dioxygen complexes are classified as side-on Peroxo ($M(O_2)$) or end-on Superoxo (MOO) to indicate the hapticity as η^2 (two atoms bounded to the metal) or η^1 (one atom bounded to the metal), respectively [6–8] (Figure 1). In this work, we have used the Quantum Theory of Atoms in Molecules (QTAIM) [9,10] for characterizing the bonding between M and O_2.

According to QTAIM, there is a bond critical point (BCP) of the electron density ($\rho(r)$) between each pair of chemical bonded atoms in a molecule [9–11]. The atomic interactions can be divided into two classes: (1) the so-called *Closed Shell* (*CS*) *Interaction* with positive value of $\nabla^2\rho(r)$ and (2) the so-called *Shared Shell* (*SS*) *Interaction* with negative value of $\nabla^2\rho(r)$ at the corresponding BCP. To further improve the characterization of the atomic interactions, Bader et al. [12] and Cremer et al. [13] proposed to evaluate some other important functions at the BCP like the kinetic energy density ($G(r)$), the potential energy density ($V(r)$) and the total energy density ($H(r)$). Bianchi et al. [14] and Espinosa et al. [15] proposed that the interactions can be sub-classified based on the value of the $|V(r)|/G(r)$ ratio at the BCP. According to them, the interactions can be separated into three groups: *Pure CS* if $0 < |V(r)|/G(r) < 1$, *Pure SS* if $|V(r)|/G(r) > 2$, and *Transit CS* if $1 < |V(r)|/G(r) < 2$.

In this letter we have performed a theoretical study on the interaction between a fourth-period transition metal atom and oxygen. We have explored the MO_n (n = 1–2) potential energy surface (PES) to determine lowest-energy geometries/configurations within the Kohn–Sham density functional theory (DFT) methodology. To classify the M–oxygen interactions, we have used a QTAIM topological analysis of $\rho(r)$ [9,10,16]. In order to find information that might be used to 'design' new complexes with similar properties, we have also performed a similarity study on the MO_n complexes using a chemotopological method [17–23]. Specifically, we carried out a chemotopological study of 40 MO_n complexes defined by 9 physico-chemical properties.

2. Computational details

All calculations in this work were performed within the unrestricted Kohn–Sham DFT methodology using the BPW91 exchange-correlation potential (U-BPW91) and the GAUSSIAN 6-311+G* basis set as implemented in the GAUSSIAN09 program [24]. Geometry optimizations were performed for several starting geometries with nuclear positions and electronic configurations

* Corresponding author.
E-mail address: emilbusuribe@usantotomas.edu.co (E.A. Uribe).

http://dx.doi.org/10.1016/j.cplett.2016.02.025
0009-2614/

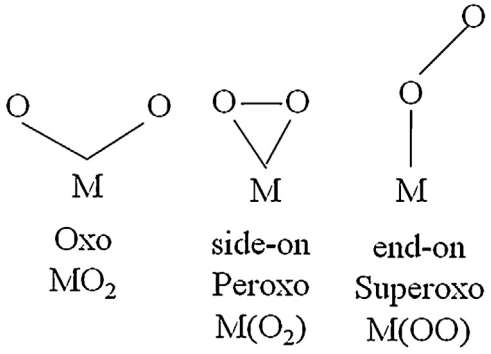

Figure 1. Classifications of M—O interactions.

(between 8 and 12 for each system) constructed by hand. All of the PES stationary points thus found were classified as local minima based on a vibrational frequency analysis. For all the complexes at the local-minimum geometry, a QTAIM analysis was performed for obtaining the topological properties of the electron density using the AIM2000 program [25] using the electron density from a single point calculation from GAUSSIAN09. Unless otherwise stated explicitly, all default settings for GAUSSIAN09 and AIM2000 programs were used.

To find the similarity relationships between MO_n complexes, a chemotopological study was performed [17–23]. Nine physicochemical properties were selected to define each one of the 40 MO_n complexes at their ground state such as: spin multiplicity, molecular weight, total and thermal energies, dipolar and quadrupolar moments, and bond length between the transition metal and oxygen ($R_{e(M-O)}$). These 9 properties might help to predict the interaction of the molecule with other molecules and solvents. Thus a 40×9 matrix was built with these values. Each property was normalized using the following relation:

$$\bar{x}_{jA} = \frac{x_{jA} - x_{\min}}{x_{j\max} - x_{j\min}} \quad (1)$$

where $\bar{x}_{jA}$ is the value of the property j of the MO_n complex A, and $x_{j\min}$ and $x_{j\max}$ are the minimum and maximum values of property j of all the MO_n complexes, respectively. Using the R package [26], a cluster analysis using 2 similarity functions and 3 clustering methodologies was performed obtaining 6 different dendrograms for the forty MO_n complexes. For each dendrogram, similarity neighborhoods were extracted to obtain a topological basis according to the procedure introduced in Refs. [17–23]. Some topological properties (closure, boundary and interior set) were calculated of different subsets of MO_n complexes such as: Early MO_n complexes = {ScO_n, TiO_n, VO_n, CrO_n}, MnO_n complexes = {MnO, MnO_2, $Mn(O_2)$, MnOO}, Late MO_n complexes = {FeO_n, CoO_n, NiO_n, CuO_n} and ZnO_n complexes = {ZnO, ZnO_2, $Zn(O_2)$, ZnOO}. The Early- and Late-MO_n classification was based on previous studies [27–29]. Because there is not currently an agreement on whether MnO_n should be considered a member of the Early set or not, we decided to considered the set MnO_n complexes = {MnO, MnO_2, $Mn(O_2)$, MnOO} as an independent set (similar reasoning applies to ZnO_n set).

3. Results

3.1. Ground state and structural properties

3.1.1. Monoxides

From Table 1, it can be seen that the spin multiplicity for the ground state increases from ScO to MnO and then decreases when moving toward ZnO. MnO has the greatest multiplicity (6) in the ground state. Notice that the energy difference between the electronic states from ScO to ZnO do not exceed 96 kcal/mol, being the early transition metal monoxides (Sc, Ti, V, Cr) the ones that have the highest energy differences (see Table 1). Table 2 shows our computed bond lengths ($R_{e(M-O)}$) and vibrational frequencies (ω_e) for the ground states of the M monoxides (MO). Some experimental and configuration interaction (CI) [30] data are also shown in Table 2 for comparison. As can be seen from Table 2, the overall difference for $R_{e(M-O)}$ is less than 0.1 Å with respect to the experimental and CI data with an average difference equal to 0.01 Å and 0.05 Å, respectively. Actually the difference between our computed and the experimental frequency value is less than 57 cm^{-1} over the whole set, the average value of this difference is equal to 19 cm^{-1}. Thus, as can be seen from Table 2, our DFT-U-BPW91/6-311+G* data is in good agreement with the experimental and CI data. Interestingly, our DFT-U-BPW91 value for $R_{e(M-O)}$ is closer to the corresponding experimental value than the CI value for some MOs. Notice that $R_{e(M-O)}$ increases going from VO to MnO, and from FeO to CuO. However, ω_e decreases going from VO to CuO except for MnO.

3.1.2. Transition metal dioxide (MO_2), peroxide ($M(O_2)$) and superoxide (MOO).

Figure 2 shows the computed M—O and O—O bond lengths and O—M—O angle of the lowest-energy isomer (potential ground state) of the M dioxides, peroxide and superoxide complexes. The energies, ΔE, ZPE, total energies including the zero-point vibrational energies and ΔE_0 for different states of all these complexes are shown in the Support Information (see Tables S1–S3).

3.1.2.1. MO_2 complexes. From Figure 2 we can see that each MO_2 is more stable than the corresponding $M(O_2)$, which, in turn, is more stable than the corresponding MOO, except for the copper complexes. Copper superoxide (CuOO) is more stable than copper dioxide (CuO_2) and peroxide $Cu(O_2)$ (see Figure 2). From Figure 2 we can also see that the spin multiplicity of the lowest-energy isomers for all transition metal dioxides is less or equal to 3 except for the MnO_2 whose value is 4. Notice that the spin multiplicity of MO_2 is reduced by 2 with respect to the corresponding MO for M = Ti-Ni (see Table 2 and Figure 2). However, ScO_2 and CuO_2 have the same spin multiplicity than ScO and CuO, respectively. The multiplicity of ZnO_2 is increased by 2 with respect to ZnO. According to the literature, the ground state for the cobalt dioxide is one the most controversial subject among the whole M dioxide series [31]. Similar to the FeO_2 anion, theoretical calculations on the Co dioxide requires sophisticated treatments [1]. In this study, we found two electronic states, $^2A_1$ and $^2\Sigma_g$, for CoO_2. A bent structure (bond angle equal to 155°) with configuration $^2A_1$ is more stable by 0.4 kcal/mol than the linear structure with $^2\Sigma_g$ configuration. Our DFT-U-BPW91/6-311+G* results are in good agreement with previous DFT calculations obtained with BP86 and B3LYP [32] functionals and in relative disagreement with CCSD(T) [33] calculations, which predict a linear geometry for CoO_2 with a $^2\Sigma^+$ state [1].

The M—O bond length in the MO_2 complexes decreases when the M atomic number increases except for of NiO_2, CuO_2 and ZnO_2 (Figure 2). Interestingly, notice that all the MO_2 complexes are bent except for NiO_2, CuO_2 and ZnO_2, which have a linear geometry. Our structures obtained at the DFT-U-BPW91/6-311+G* level of theory are in good agreement with the ones obtained at BP86/6-31+G* level for ScO_2 [34]; B3LYP level for TiO_2, VO_2, CrO_2, MnO_2, FeO_2 and ZnO_2 [35–40]; CASSCF level for CoO_2 [32]; and LSDA-VWN/DZVP level for NiO_2 [41].

3.1.2.2. $M(O_2)$ and MOO complexes. The spin multiplicity of each MOO is equal to the corresponding $M(O_2)$, except for CoOO and

Table 1
Energies (hartree), relative stabilities (ΔE) (kcal/mol), zero-point vibrational energies (ZPE), total energies including the zero-point vibrational energies (hartree) and relative stabilities including the zero-point vibrational energies (ΔE_0) (kcal/mol) for different states or multiplicities (M) of the transition metal monoxides calculated using UBPW91 functional and 6-311+G* basis sets.

MO	**ScO**		**TiO**		**VO**		
Multiplicity	2	4	3	5	2	4	6
Energy	−836.001578	−835.862914	−924.752731	−924.599120	−1019.275448	−1019.301816	−1019.151355
ΔE	0.0	87.0	0.0	96.4	16.5	0.0	94.4
ZPE	0.002214	0.001477	0.002312	0.001559	0.002404	0.002314	0.001449
Total energy	−835.999364	−835.861437	−924.750419	−924.597561	−1019.273044	−1019.299502	−1019.149906
ΔE_0	0.0	86.6	0.0	95.9	16.6	0.0	93.9
MO	**CrO**			**MnO**			
Multiplicity	3	5	7	2	4	6	8
Energy	−1119.723145	−1119.765740	−1119.691774	−1226.227400	−1226.254655	−1226.308050	−1226.226509
ΔE	26.7	0.0	46.4	50.6	33.5	0.0	51.2
ZPE	0.002170	0.002076	0.001323	0.002205	0.002111	0.002043	0.001210
Total energy	−1119.720975	−1119.763664	−1119.690451	−1226.225195	−1226.252544	−1226.306007	−1226.225299
ΔE_0	26.8	0.0	45.9	50.7	33.5	0.0	50.6
MO	**FeO**		**CoO**			**NiO**	
Multiplicity	5	7	2	4	6	3	5
Energy	−1339.017421	−1338.977542	−1458.044827	−1458.065667	−1458.033846	−1583.624754	−1583.569158
ΔE	0.0	25.0	13.1	0.0	20.0	0.0	34.9
ZPE	0.002068	0.001813	0.002065	0.001942	0.001776	0.001873	0.00174
Total energy	−1339.015353	−1338.975729	−1458.042762	−1458.063725	−1458.032070	−1583.622881	−1583.567418
ΔE_0	0.0	24.9	13.2	0.0	19.9	0.0	34.8
MO	**CuO**		**ZnO**				
Multiplicity	2	4	1	3			
Energy	−1715.804156	−1715.748150	−1854.630744	−1854.622524			
ΔE	0.0	35.1	0.0	5.2			
ZPE	0.001498	0.001276	0.001694	0.001067			
Total energy	−1715.802658	−1715.746874	−1854.629050	−1854.621457			
ΔE_0	0.0	35.0	0.0	4.8			

Table 2
Bond lengths between Transition Metal and Oxygen ($R_{e(M-O)}$, in Å) and vibrational frequencies (ω_e, in cm^{-1}) of the ground state Transition Metal Monoxides.

Properties	3D-M oxides									
	ScO	TiO	VO	CrO	MnO	FeO	CoO	NiO	CuO	ZnO
Spin multiplicity in the ground state	2	3	4	5	6	5	4	3	2	1
R_e (M—O)	1.666	1.618	1.587	1.611	1.629	1.608	1.636	1.639	1.734	1.714
CI[a]	1.657	1.598	1.553	1.584	1.734	1.695	1.652	1.682	1.821	1.746
Experimental	1.668[h]	1.620[c]	1.592[h]	1.615[e]	1.648[h]	1.619[h]	1.631[h]	1.631[h]	1.730[f]	
ω_e	972	1015	1016	911	897	908	853	822	657	743
Experimental	1000[b]	1009[c]	1011[g]	898.4[e]	840[g]	880[g]	853[g]	838[g]	640[d]	

[a] M. Dolg, U. Wedig, H. Stoll, H. J. Preuss, Chem. Phys. 86 (1987) 2123.
[b] H. Wu, L.-S. Wang, J. Phys. Chem. A 102 (1998) 9129.
[c] Z.-W. Qu, G.-J. Kroes, J. Phys. Chem. B 110 (2006) 8998.
[d] H. Wu, S.R. Desai, L.-S. Wang, J. Phys. Chem. A 101 (1997) 2103.
[e] T.C. Steimle, D.F. Nachman, J.E. Shirley, J. Chem. Phys. 91 (1989) 2049.
[f] X. Zhuang, S.E. Frey, T.C. Steimle, J. Chem. Phys. 132 (2010) 234312.
[g] C.W. Bauschlicher, Jr. P. Maitre, Theor. Chim. Acta 90 (1995) 189.
[h] E.G. Bakalbassis, M.-A.D. Stiakaki, A.C. Tsipis, C.A. Tsipis, Chem. Phys. 205 (1996) 389.

NiOO complexes, which have a lower spin multiplicity by two units than $Co(O_2)$ and $Ni(O_2)$, respectively. If we compare the ground state of transition metal peroxide and superoxide, we can see that each complex has the same spin multiplicity in the ground-state as the corresponding transition metal monoxide (see Figure 2 and Table 2), except for CoOO ($^2A'$) and NiOO complex ($^1A'$). Notice that the transition metal form complexes with low spin multiplicity, while the peroxo and the superoxo form complexes with high spin multiplicity (Figure 2). Notice also that the energy difference between the transition metal dioxide and their corresponding peroxides and superoxides decreases from the TiO_2 until ZnO_2, except for FeO_2. The energy difference between the FeO_2 and $Fe(O_2)$ is equal to 58 kcal/mol, and with the FeOO is equal to 68 kcal/mol.

According to Figure 2, the M—O ($R_{e(M-O)}$) and O—O ($R_{e(O-O)}$) bond lengths in the $M(O_2)$ are larger than in the corresponding MOO. For the $M(O_2)$s, the bond length $R_{e(M-O)}$ is in the range 1.774–1.911 Å, $R_{e(O-O)}$ is in the range 1.377–1.730 Å. For the MOOs, the bond length $R_{e(M-O)}$ is in the range 1.702–1.899 Å, $R_{e(O-O)}$ is in the range 1.296–1.388 Å. Our values are in partial agreement with those reported previously by Gutsev et al. [8] who reported the O—O distance in the $M(O_2)$ and MO_2 complexes is in the range 1.4–1.55 Å and 2.5–2.8 Å, respectively, and around 1.3 Å in the MOO complexes. Notice also that MOO has a greater angle than the corresponding $M(O_2)$. Actually, from Figure 2 we can see that early transition metal (Sc, Ti, V and Cr) superoxides have linear geometry except for CrOO (M—O—O angle equal to 100°). However, the late transition metal (Fe, Co, Ni and Cu) superoxides have bent structure.

3.2. Transition metal–oxygen interactions in MO_n complexes

Within the QTAIM formalism, we have analyzed the nature of the M—O and O—O interactions based on the values of the electron density $\rho(r)$, its Laplacian ($\nabla^2\rho(r)$), the kinetic energy density ($G(r)$),

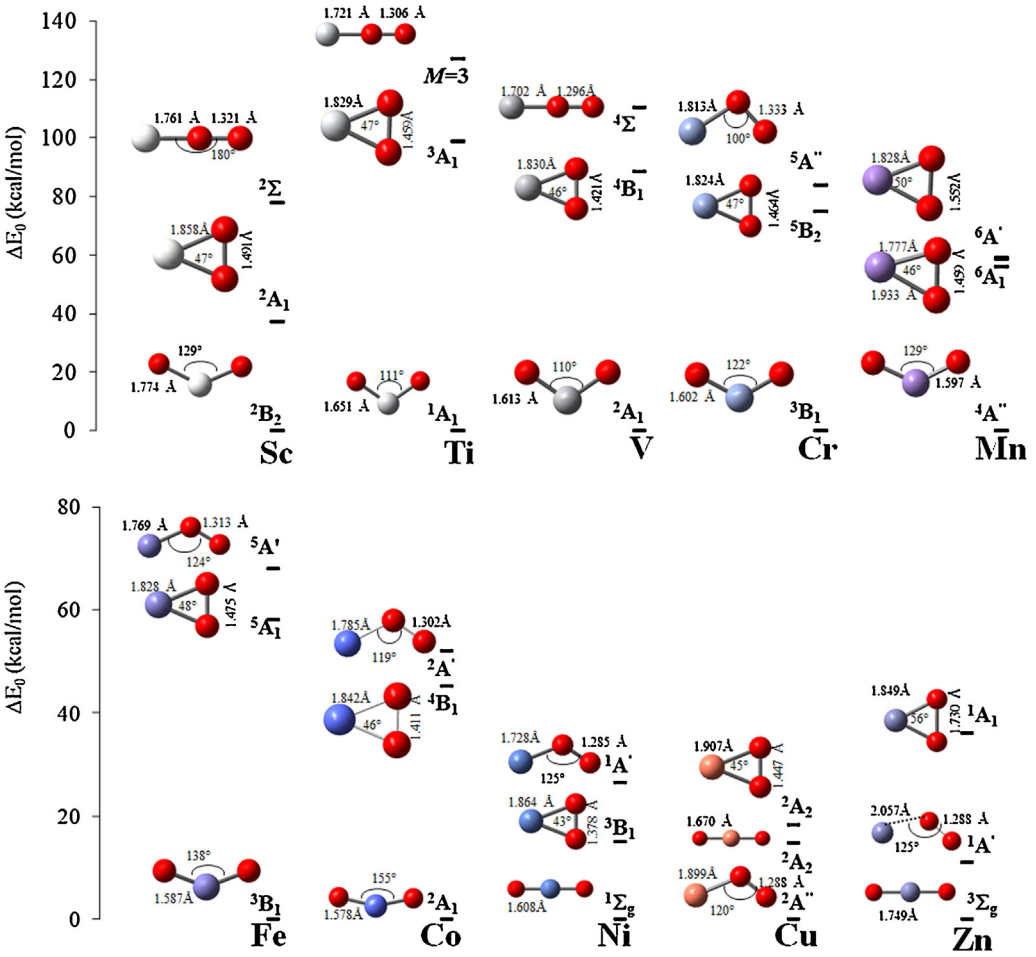

Figure 2. Energies (in kcal/mol) of transition metal peroxide and superoxide complexes given with respect to the total energy of the ground state of each particular dioxide.

the potential energy density ($V(r)$) and the total energy density ($H(r)$), evaluated at the corresponding BCP (see Table 3). According to the positive values of $\nabla^2\rho(r)$ (see Table 3), all M—O bonds can be classified as *Closed Shell* (*CS*). The O—O bond in MO_n complexes can be of two types: *Closed Shell* ($\nabla^2\rho(r)>0$) in the M peroxo complexes and *Shared Shell* ($\nabla^2\rho(r)<0$) in the M superoxo complexes. Nevertheless, we found one exception to this classification. In the Mn superoxo complex the $\nabla^2\rho(r)$ values for the O—O bonds are small but positive indicating a *CS* interaction. The negative value of $H(r)$ for all M—O and O—O bonds indicates a stabilizing and attractive interaction [42]. As mentioned above, the *CS* interactions are sub-divided in *Transit CS* and *Pure CS* interactions [14,15,43–45]. According to the value of the $|V(r)|/G(r)$ ratio, from Table 3 we can see that the M—O bond in all MO_n complexes are classified as *Transit CS* ($1<|V(r)|/G(r)<2$). The O—O bond in the all M peroxides and in MnOO complex is also classified as *Transit CS*.

The cyclic nature of the M peroxo complexes is confirmed by the occurrence of a ring critical point (RCP) according to QTAIM (see Table 3). Interestingly, our calculations show that the MnOO complex has also a cyclic structure. The MnOO complex has different geometrical features than $Mn(O_2)$ though (the lowest-energy isomer of MnOO ($^6A'$) is 1.87 kcal/mol more stable that the one of $Mn(O_2)$ ($^6A_1$)). The Mn—O bonds in the MnOO complex has different length (Mn—O1 = 1.777 Å and Mn—O_2 = 1.933 Å), however they have same length in the $Mn(O_2)$ complex (Mn—O1 = Mn—O_2 = 1.828 Å). The values of $\rho(r)$ at the BCP corresponding to each Mn—O bonds in the MnOO complex indicate that the Mn—O1 bond has a higher covalence degree than in the Mn—O bonds in the $Mn(O_2)$ complex. It is worth mentioning that we did not find a BCP between Zn and O_2 ligand in the ZnOO complex (bond length Zn—O is 2.057 Å).

3.3. *Chemotopological analysis of MO_n complexes*

The set of the MO_n complexes is composed of 40 complexes where each one is a local minimum of the PES (10 MO complexes, 10 MO_2 complexes, 10 $M(O_2)$ complexes, and 10 MOO complexes). Each one of these complexes is defined by 9 physico-chemical properties. In order to find similarities between the MO_n complexes we performed 6 cluster analysis using 2 similarity functions (Euclidean and Manhattan distance) and 3 grouping methodologies (single, complete and average) based on previous studies [17]. For each one of them a dendrogram was obtained. Clusters and their population were determined using the Restrepo et al. methodology [17–22]. The number of sets considered, m, is equal to the integer number that maximizes the selection number S ($S=S(m)$), which in turn guarantees a maximum number of sets with high population (see Refs. [17–22]). Once the value of is m thus determined, the B_m topological basis is built for each dendrogram (Fig. S1–S6 in Support Information). The 6 dendrograms obtained do not vary considerably. Each dendrogram has groups of elements belonging of the Early MO_n set and groups belonging to the Late MO_n set. The MnO_n complexes are grouped with some CrO_n and FeO_n complexes; the ZnO_n with some CuO_n and NiO_n complexes. Since the dendrograms are quite similar, we decided to choose only one representative dendrogram in our similarity study. This representative dendrogram is the one obtained considering the Euclidean distance

Table 3
Laplacian of the charge density ($\nabla^2\rho(r)$), $|V(r)|/G(r)$ ratio where $G(r)$ is kinetic energy density and $V(r)$ is potential energy density, total energy density ($H(r)$) and Bond Degree (BD = $H(r)/\rho(r)$) at the BCP (3,−1) for the M—O and O—O bonds calculated using UBPW91/6-311+G* level of theory.

MO_n	Interaction	Description	$\rho(r)$ (a.u.)	$\nabla^2\rho(r)$ (a.u.)	$\lvert V(r)\rvert/G(r)$	$H(r)$ kcal/mol	$H(r)/\rho(r)$	*Re* (Å)
ScO	Sc—O	(3,−1)	0.241	0.190	1.432	−377.565	−1566.660	1.666
TiO	Ti—O	(3,−1)	0.266	0.210	1.460	−466.357	−1753.221	1.618
VO	V—O	(3,−1)	0.280	0.220	1.474	−529.357	−1890.561	1.587
CrO	Cr—O	(3,−1)	0.254	0.220	1.444	−453.907	−1787.035	1.611
MnO	Mn—O	(3,−1)	0.234	0.200	1.420	−386.118	−1650.077	1.629
FeO	Fe—O	(3,−1)	0.240	0.220	1.403	−391.975	−1633.229	1.608
CoO	Co—O	(3,−1)	0.214	0.260	1.297	−287.252	−1342.299	1.636
NiO	Ni—O	(3,−1)	0.203	0.280	1.249	−240.595	−1185.197	1.639
CuO	Cu—O	(3,−1)	0.151	0.210	1.155	−100.582	−666.106	1.734
ZnO	Zn—O	(3,−1)	0.146	0.190	1.163	−97.766	−669.630	1.714
ScO_2	Sc—O	(3,−1)	0.170	0.170	1.300	−186.756	−1098.565	1.774
TiO_2	Ti—O	(3,−1)	0.243	0.200	1.429	−395.809	−1628.844	1.651
VO_2	V—O	(3,−1)	0.262	0.220	1.447	−475.151	−1813.553	1.613
CrO_2	Cr—O	(3,−1)	0.262	0.230	1.443	−481.648	−1838.351	1.602
MnO_2	Mn—O	(3,−1)	0.259	0.240	1.429	−473.356	−1827.629	1.597
FeO_2	Fe—O	(3,−1)	0.257	0.260	1.399	−459.160	−1786.615	2.587
CoO_2	Co—O	(3,−1)	0.254	0.300	1.362	−440.156	−1732.898	2.578
NiO_2	Ni—O	(3,−1)	0.226	0.340	1.269	−327.289	−1448.181	1.608
CuO_2	Cu—O	(3,−1)	0.184	0.280	1.197	−116.151	−631.255	1.670
ZnO_2	Zn—O	(3,−1)	0.148	0.200	1.154	−96.622	−652.851	1.749
$Sc(O_2)$	Sc—O1	(3,−1)	0.142	0.130	1.274	−129.220	−910.000	1.858
	Sc—O2	(3,−1)	0.142	0.130	1.274	−129.220	−910.000	1.858
	O1—O2	(3,−1)	0.242	0.060	1.699	−357.163	−1475.880	1.491
	O—Sc—O	(3,+1)	0.101	0.160	1.038	−16.533	−163.744	–
$Ti(O_2)$	Ti—O1	(3,−1)	0.131	0.150	1.102	−44.069	−336.405	1.829
	Ti—O2	(3,−1)	0.131	0.150	1.102	−44.069	−336.405	1.829
	O1—O2	(3,−1)	0.317	0.130	1.505	−337.588	−1064.946	1.459
	O—Ti—O	(3,+1)	0.130	0.134	1.085	−32.705	−251.137	–
$V(O_2)$	V—O1	(3,−1)	0.140	0.150	1.253	−129.158	−922.557	1.830
	V—O2	(3,−1)	0.140	0.150	1.253	−129.158	−922.557	1.830
	O1—O2	(3,−1)	0.297	0.030	1.871	−548.916	−1848.202	1.421
	O—V—O	(3,+1)	0.106	0.182	1.035	−17.339	−164.009	–
$Cr(O_2)$	Cr—O1	(3,−1)	0.140	0.140	1.257	−125.926	−899.471	1.824
	Cr—O2	(3,−1)	0.140	0.140	1.257	−125.926	−899.471	1.824
	O1—O2	(3,−1)	0.263	0.050	1.779	−427.501	−1625.479	1.464
	O—Cr—O	(3,+1)	0.103	0.175	1.021	−9.889	−95.758	–
$Mn(O_2)$	Mn—O1	(3,−1)	0.135	0.150	1.215	−108.633	−804.689	1.828
	Mn—O2	(3,−1)	0.135	0.150	1.215	−108.633	−804.689	1.828
	O1—O2	(3,−1)	0.207	0.070	1.571	−246.980	−1193.140	1.552
	O—Mn—O	(3,+1)	0.096	0.153	1.002	−0.765	−7.975	–
$Fe(O_2)$	Fe—O1	(3,−1)	0.132	0.160	1.181	−91.333	−691.917	1.828
	Fe—O2	(3,−1)	0.132	0.160	1.181	−91.333	−691.917	1.828
	O1—O2	(3,−1)	0.255	0.050	1.755	−401.531	−1574.631	1.475
	O—Fe—O	(3,+1)	0.098	0.167	0.991	3.756	38.402	–
$Co(O_2)$	Co—O1	(3,−1)	0.119	0.160	1.132	−108.204	−909.277	1.842
	Co—O2	(3,−1)	0.119	0.160	1.132	−108.204	−909.277	1.842
	O1—O2	(3,−1)	0.281	0.160	1.840	−706.928	−2515.758	1.411
	O—Co—O	(3,+1)	0.114	0.218	1.008	−4.793	−42.099	–
$Ni(O_2)$	Ni—O1	(3,−1)	0.121	0.150	1.050	−20.621	−170.421	1.864
	Ni—O2	(3,−1)	0.121	0.150	1.050	−20.621	−170.421	1.864
	O1—O2	(3,−1)	0.396	0.150	1.557	−489.557	−1236.255	1.378
	O—Ni—O	(3,+1)	0.121	0.140	1.037	−14.016	−116.276	–
$Cu(O_2)$	Cu—O1	(3,−1)	0.094	0.120	1.096	−33.063	−351.734	1.907
	Cu—O2	(3,−1)	0.095	0.120	1.097	−33.615	−353.842	1.907
	O1—O2	(3,−1)	0.277	0.030	1.848	−474.238	−1712.051	1.447
	O—Cu—O	(3,+1)	0.066	0.100	0.994	1.509	22.868	–
$Zn(O_2)$	Zn—O1	(3,−1)	0.110	0.140	1.124	−52.398	−476.345	1.849
	Zn—O2	(3,−1)	0.110	0.140	1.124	−52.398	−476.345	1.849
	O1—O2	(3,−1)	0.130	0.070	1.242	−59.446	−457.277	1.730
	O—Zn—O	(3,+1)	0.077	0.096	1.036	−9.426	−123.064	–
ScOO	Sc—O1	(3,−1)	0.148	0.230	1.158	−113.276	−765.378	1.761
	O1—O2	(3,−1)	0.376	−0.020	2.061	−878.789	−2337.205	1.321
TiOO	Ti—O1	(3,−1)	0.160	0.250	1.180	−143.778	−898.613	1.721
	O1—O2	(3,−1)	0.393	−0.030	2.097	−952.789	−2424.399	1.306
VOO	V—O1	(3,−1)	0.165	0.260	1.193	−160.395	−972.091	1.702
	O1—O2	(3,−1)	0.405	−0.040	2.128	−1009.318	−2492.143	1.296
CrOO	Cr—O1	(3,−1)	0.147	0.150	1.259	−136.341	−927.490	1.813
	O1—O2	(3,−1)	0.376	−0.020	2.075	−866.087	−2303.423	1.833
MnOO	Mn—O1	(3,−1)	0.156	0.150	1.278	−156.332	−1002.128	1.777
	Mn—O2	(3,−1)	0.102	0.120	1.121	−45.157	−442.716	1.933
	O1—O2	(3,−1)	0.267	0.050	1.788	−441.637	−1654.071	1.459
	O—Mn—O	(3,+1)	0.092	0.154	0.996	1.731	18.905	–

Table 3 (*Continued*)

MO_n	Interaction	Description	$\rho(r)$ (a.u.)	$\nabla^2\rho(r)$ (a.u.)	$\lvert V(r)\rvert/G(r)$	$H(r)$ kcal/mol	$H(r)/\rho(r)$	*Re* (Å)
FeOO	Fe—O1	(3,−1)	0.151	0.170	1.222	−129.047	−854.616	1.769
	O1—O2	(3,−1)	0.393	−0.030	2.107	−943.654	−2401.155	1.313
CoOO	Co—O1	(3,−1)	0.141	0.180	1.163	−114.080	−809.078	1.785
	O1—O2	(3,−1)	0.410	−0.050	2.145	−661.669	−1613.827	1.302
NiOO	Ni—O1	(3,−1)	0.156	0.240	1.156	−114.893	−736.494	1.728
	O1—O2	(3,−1)	0.429	−0.060	2.168	−1109.033	−2585.159	1.285
CuOO	Cu—O1	(3,−1)	0.098	0.130	1.076	−28.257	−288.337	1.899
	O1—O2	(3,−1)	0.425	−0.060	2.184	−1092.137	−2569.734	1.288
ZnOO	O1—O2	(3,−1)	0.424	−0.060	2.175	1088.026	2566.099	1.288

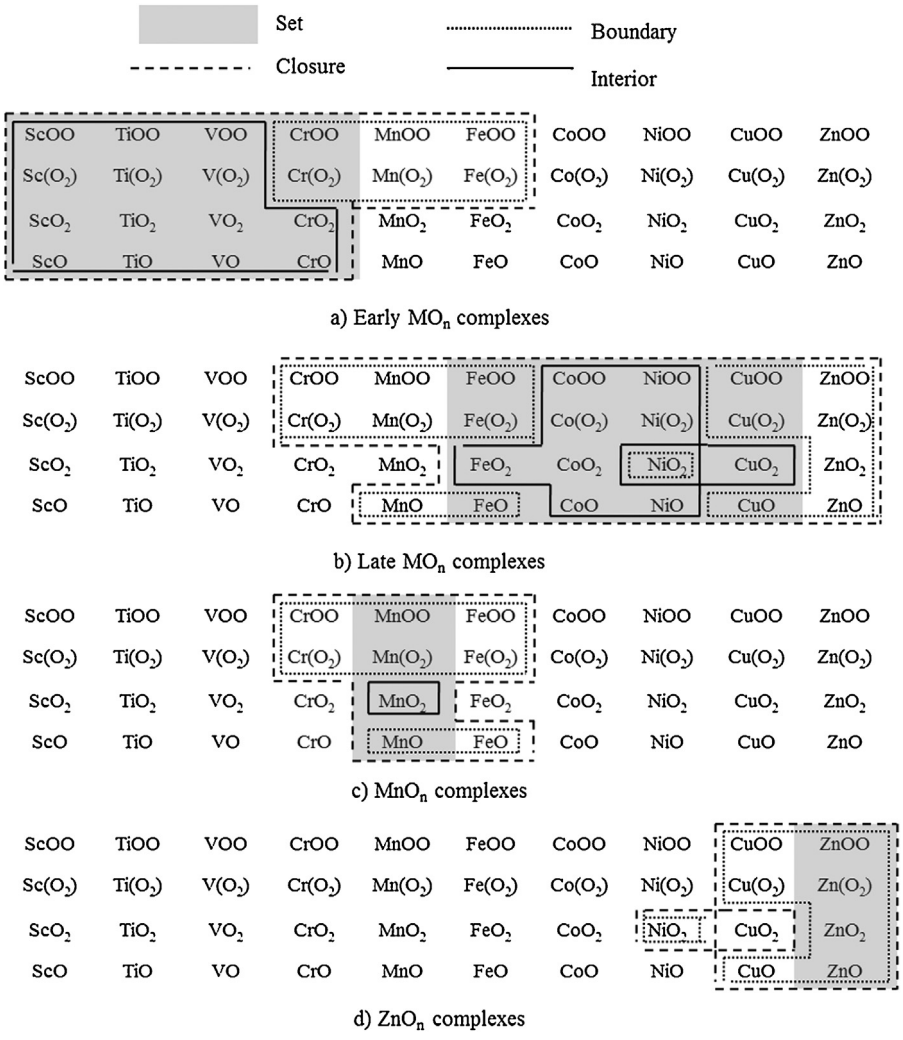

Figure 3. Topological properties of the set of: (a) Early MO_n complexes, (b) Late MO_n complexes, (c) MnO_n complexes and (d) ZnO_n complexes.

and the complete grouping methodology is shown in Fig. S1. For this case the value of *m* is equal to 4, thus its topological basis is B_4:

$$B_4\left\{\begin{array}{l}\{Cu(O_2), Zn(O_2)\}, \{CuOO, ZnOO\}, \{NiO_2, ZnO_2\}, \{CoOO, NiOO\}, \{CuO_2, FeO_2, CoO_2\},\\ \{CuO, ZnO\}, \{ScO, TiO\}, \{CoO, NiO\}, \{MnO, FeO\}, \{VO, CrO\}, \{MnO_2\},\\ \{TiOO, VOO, Ti(O_2), V(O_2)\}, \{Co(O_2), Ni(O_2)\}, \{CrOO, MnOO, FeOO\},\\ \{Mn(O_2), Cr(O_2), Fe(O_2)\}, \{Sc(O_2), ScOO\}, \{VO_2, CrO_2\}, \{ScO_2, TiO_2\}\end{array}\right\} \quad (2)$$

Based on this topological basis we studied some subsets of the MO_n complexes and their topological properties.

Early MO_n complexes = $\{ScO_n, TiO_n, VO_n, CrO_n\}$. The closure set suggests an existence of topological relationships between these complexes and Fe & Mn peroxide and superoxide (Figure 3). The boundary set shows that the early MO_n complexes have no relation with CoO_n, NiO_n, CuO_n and ZnO_n, and the interior set contains all ScO_n, TiO_n, VO_n, and chromium monoxide and dioxide whose properties are closely related only with the early MO_n complexes [46,47].

Late MO_n complexes = {FeO_n, CoO_n, NiO_n, CuO_n}. The closure of the set is formed of all Late MO_n complexes along with CrOO, $Cr(O_2)$, MnOO, $Mn(O_2)$ and MnO complexes (Figure 3). The interior of this set is formed of all CoO_n and NiO_n (except NiO_2), CuO_2 and FeO_2 complexes. It is important to notice that this set does not appear related to ScO_n, TiO_n and VO_n complexes. Thus our results show that the similarity relations between the elements of group VIIIB (Fe, Co and Ni) are transferred to their corresponding MO_n complexes. Notice that these complexes not only have similarity relations among themselves but also with CuO_2. It is worth mentioning that these similarity relations obtained theoretically might predict oxides that could be used in corrosion processes where their similar oxides are used [32,48]. More studies are needed to confirm this relation. It is important to keep in mind that this particular result was obtained using only 9 physico-chemical properties.

MnO_n complexes = {MnO, MnO_2, $Mn(O_2)$, MnOO}. The boundary, closure and interior sets of MnO_n complexes suggest that there are not topological relations between MnO_n complexes and the other complexes corresponding to elements that are far away in the periodic table such as ScO_n, TiO_n, VO_n, CoO_n, NiO_n, CuO_n and ZnO_n. The MnO_n complexes have only similarity relations with some CrO_n and FeO_n complexes, that is, Mn peroxide/superoxide only have similarity relations with the peroxide/superoxide of the 'neighbors' elements of Mn (Cr and Fe) on the periodic table. The boundary and closure sets also show similarity relationships between the MnO and FeO. These results might indicate that the Mn oxides, whom industrial use has not been well explored yet, could have a chemical behavior similar to that of Fe and Cr oxides [49]. However, this can only be verified with the synthesis of these complexes and testing.

ZnO_n complexes = {ZnO, ZnO_2, $Zn(O_2)$, ZnOO}. The closure and boundary of this set have NiO_2 and all CuO_n complexes, except CuO_2 complex (Figure 3). Thus, ZnO_n complexes are more related to some CuO_n complexes and NiO_n complexes than those Early MO_n and MnO_n complexes. So our study shows similarity relations between ZnO and CuO_n & NiO_n.

4. Conclusions

A partial search of the PES for the transition metal monoxide (MO), dioxide (MO_2), peroxide ($M(O_2)$) and superoxide (MOO) was performed at the DFT-U-BPW91/6-311+G* level of theory. It was found that the M dioxide is more stable than the corresponding peroxide and superoxide, except for CuO_2, and that M dioxide forms complexes with low spin multiplicity, while the peroxo and the superoxo form complexes with high spin multiplicity.

Using QTAIM we have analyzed the bonding of the MO_n complexes (n = 1–2). According to QTAIM, M—O bonds can be classified as *Closed Shell* (*CS*) for any MO_n complex. The O—O bond in MO_n complexes can be of two types: *Closed Shell* ($\nabla^2\rho(r) > 0$) in the M peroxo complexes and *Shared Shell* ($\nabla^2\rho(r) < 0$) in the M superoxo complexes (except for MnOO for which the O—O bond is *CS*). Based on the $|V(r)|/G(r)$ ratio value, the M—O bond in all MO_n complexes is classified as *Transit CS* ($1 < |V(r)|/G(r) < 2$). The O—O bond in the all M peroxides and in MnOO complex is also classified as *Transit CS*. Our QTAIM analysis predicts that all the M peroxides ($M(O_2)$) and, interestingly, the MnOO complex are cyclic as indicated by the presence of a ring critical point.

As far as we know, by the first time, a chemotopological classification of the 40 MO_n complexes based on nine of their physico-chemical properties was performed for determining similarity relations. The fourth-period MO_n (n = 1–2) was classified into four sets: early MO_n complexes, MnO_n complexes, Late MO_n complexes and ZnO_n complexes. The early MO_n complexes have similarity relations with some MnO_n and FeO_n complexes. However, they do not have similarity relations with neither the Late MO_n complexes nor the ZnO_n complexes. The MnO_n complexes only have similarity relations with some CrO_n, and FeO_n complexes. No similarity relations could be determined between the Late MO_n and the ScO_n, TiO_n and VO_n complexes. The ZnO_n complexes are related with some CuO_n complexes and with NiO_2. These similarity relations obtained theoretically might predict oxides that could be used in the industrial processes where their similar oxides are used [1,32,46–49].

Acknowledgements

We thank Universidad Santo Tomás (Projects FODEIN-2013-82, FODEIN-2014-1 and FODEIN-2015-110000101-004) for the financial support. We gratefully acknowledge CPU time from the Sharcnet Computer Project, Ontario, Canada, where most of the calculations were performed, and Prof. Paul Ayers, at McMaster University, Hamilton, Ontario, Canada. JIR thanks SIP-IPN (project 20161594) for financial support.

Appendix A. Supplementary data

Supplementary data associated with this article can be found, in the online version, at doi:10.1016/j.cplett.2016.02.025.

References

[1] Y. Gong, M. Zhou, L. Andrews, Chem. Rev. 109 (2009) 6765.
[2] M. Costas, M.P. Mehn, M.P. Jensen, L. Que Jr., Chem. Rev. 104 (2004) 939.
[3] J.F. Weaver, Chem. Rev. 113 (2013) 4164.
[4] L.M. Mirica, X. Ottenwaelder, T.D.P. Stack, Chem. Rev. 104 (2004) 1013.
[5] E.A. Lewis, W.B. Tolman, Chem. Rev. 104 (2004) 1047.
[6] M. Suzuki, Acc. Chem. Res. 40 (2007) 609.
[7] P.L. Holland, Dalton Trans. 39 (2010) 5415.
[8] G.L. Gutsev, B.K. Rao, P. Jena, J. Phys. Chem. A 104 (2000) 11961.
[9] R.F.W. Bader, Atoms in Molecules. A Quantum Theory, Oxford University Press, Oxford, 1990.
[10] C.F. Matta, R.J. Boyd (Eds.), The Quantum Theory of Atoms in Molecules. From Solid State to DNA and Drug Design, Wiley-VCH, Weinheim, 2007.
[11] R.F.W. Bader, J. Phys. Chem. A 102 (1998) 7314.
[12] R.F.W. Bader, H. Essén, J. Chem. Phys. 80 (1984) 1943.
[13] D. Cremer, E. Kraka, Croat. Chem. Acta 57 (1984) 1259.
[14] R. Bianchi, G. Gervasio, D. Marabello, C. R. Chim. 8 (2005) 1392.
[15] E. Espinosa, I. Alkorta, J. Elguero, E. Molins, J. Chem. Phys. 117 (2002) 5529.
[16] J.I. Rodríguez, J. Comp. Chem. 34 (2013) 681.
[17] G. Restrepo, H. Mesa, E.J. Llanos, J.L. Villaveces, J. Chem. Inf. Comput. Sci. 44 (2004) 68.
[18] G. Restrepo, J.L. Villaveces, Croat. Chem. Acta 78 (2005) 275.
[19] G. Restrepo, E.J. Llanos, H. Mesa, J. Math. Chem. 39 (2006) 401.
[20] G. Restrepo, H. Mesa, J.L. Villaveces, J. Math. Chem. 39 (2006) 363.
[21] G. Restrepo, H. Mesa, Curr. Comput. Aid Drug. 7 (2011) 90.
[22] N. Quintero, G. Restrepo, I.M. Cohen, J. Radioanal. Nucl. Chem. 295 (2013) 823.
[23] M.C. Daza, G. Restrepo, E.A. Uribe, J.L. Villaveces, Chem. Phys. Lett. 428 (2006) 55.
[24] M.J. Frisch, et al., Gaussian 09, Revision B.01, Gaussian, Inc., Wallingford, CT, 2009.
[25] F. Biegler-König, J. Schönbohm, D.J. Bayles, J. Comput. Chem. 22 (2001) 545.
[26] R Development Core Team, A Language and Environment for Statistical Computing. R Foundation for Statistical Computing, Vienna, Austria, 2011.
[27] N.B. Balabanov, K.A. Peterson, J. Chem. Phys. 123 (2005) 064107.
[28] J.I. Van der Vlugt, Eur. J. Inorg. Chem. 2012 (2012) 363.
[29] E.A. Carter, W.A. Goddard III, J. Phys. Chem. 92 (1988) 2109.
[30] M. Dolg, U. Wedig, H. Stoll, H. Preuss, J. Chem. Phys. 86 (1987) 2123.
[31] E.L. Uzunova, H. Mikosch, G. St. Nikolov, J. Chem. Phys. 128 (2008) 094307.
[32] G.V. Chertihin, A. Citra, L. Andrews, C.W. Bauschlicher Jr., J. Phys. Chem. A 101 (1997) 8793.
[33] D. Danset, M.E. Alikhani, L. Manceron, J. Phys. Chem. A 109 (2005) 105.
[34] G.V. Chertihin, L. Andrews, M. Rosi, C.W. Bauschlicher Jr., J. Phys. Chem. A 101 (1997) 9085.
[35] G.V. Chertihin, W.D. Bare, L. Andrews, J. Phys. Chem. A 101 (1997) 5090.
[36] G.V. Chertihin, W.D. Bare, L. Andrews, J. Chem. Phys. 107 (1997) 2798.
[37] G.V. Chertihin, L. Andrews, J. Phys. Chem. A 101 (1997) 8547.
[38] M.B. Walsch, R.A. King, H.F. Schaefer III, J. Chem. Phys 110 (1999) 5224.
[39] L. Andrews, G.V. Chertihin, A. Ricca, C.W. Bauschlicher Jr., J. Am. Chem. Soc. 118 (1996) 467.
[40] G.V. Chertihin, L. Andrews, J. Chem. Phys. 106 (1997) 3457.
[41] A. Citra, G.V. Chertihin, M. Neurock, L. Andrews, J. Phys. Chem. A 101 (1997) 3109.

[42] J.A. Dobado, H. Martínez-García, J. Molina, M.R. Sundberg, J. Am. Chem. Soc. 120 (1998) 8461.
[43] E.A. Uribe, M.C. Daza, J.L. Villaveces, Chem. Phys. Lett. 490 (2010) 143.
[44] R. Bianchi, G. Gervasio, D. Marabello, Inorg. Chem. 39 (2000) 2360.
[45] E.A. Uribe, M.C. Daza, J.L. Villaveces, S.A. Delgado, Int. J. Quant. Chem. 110 (2010) 524.
[46] Y. Zhao, Y. Gong, M. Chen, M. Zhou, J. Phys. Chem. A 110 (2006) 1845.
[47] Z.-W. Qu, G.-J. Kroes, J. Phys. Chem. B 110 (2006) 8998.
[48] G.E. Johnson, J.U. Reveles, N.M. Reilly, E.C. Tyo, S.N. Khanna, A.W. Castleman Jr., J. Phys. Chem. A 112 (2008) 11330.
[49] G.L. Gutsev, C.A. Weatherford, K. Pradhan, P. Jena, J. Phys. Chem. A 114 (2010) 9014.